中國機械工程學刊第三十四卷第四期第 331~340 頁(民國一百零二年)
Journal of the Chinese Society of Mechanical Engineers, Vol.34, No.4, pp331~340 (2013)

# Finite-Element Analysis of the Lateral Compression of Clad Tube between V-Shaped Dies

Tsung-Chia Chen* and Jiun-Ming Ye**

**Keywords** : elastic-plastic, clad tube, squaring, collapse.

## ABSTRACT

The lateral compression of clad tubes owing to a large deformation is examined by an incremental elastic-plastic finite-element method based on an updated Lagrangian formulation, in which a sliding-sticking friction mode is specially considered. It is mainly expected to predict the collapse of clad tubes and the asymmetry of clad tubes during the design stage, before trials. The effects of various parameters in the process, such as geometric ratio *R/t*, friction coefficient $\mu$ and strain hardening exponent *n*, on the occurrence of collapse and asymmetry of tube are discussed and interpreted in simulations. The findings show that geometric ratio is the major factor in the process of squaring circular tubes. When *R/t*=25, serious collapse is likely to appear. Aiming at circular tubes with geometric ratio *R/t*=25, this study proposes six analysis configurations for clad tubes to discuss the possibility of clad tubes avoiding collapse. The findings showed that clad tubes could effectively reduce the collapse ratio and enhance the symmetry of square tubes. The present work may be expected to improve the understanding of the collapse mechanism of lateral compression.

## INTRODUCTION

Tubular products are widely applied in various industries. In particular, seamless tubing, which is usually made by piercing and extrusion, is used in high-temperature or high-pressure applications as well as for transporting gas or chemical liquids. There are several methods of exerting pressure according to the location of tube, such as shaping at tube end (Zhang et al., 2010; Lin et al., 2010; Miscow et al., 1997; Leu, 2000; Huang, 2005; Yu et al., 2005) or pressing circular tube with two rigid (Reid et al., 1983; Watson et al., 1976; Watson et al., 1976; Johnson et al., 1977), parallel plates on both sides of the tube for the occurrence of the character of circular tube collapse, energy absorbing method for the application of circular tube (Mutchler , 1960; DeRuntz et al., 1963; Reid et al., 1978; Gotoh et al., 1989), and Leu (2006) for the influence of the parameter on squaring circular tube simply with finite element method.

This study conducted radially compressed press-forming to the clad tube between two V-shape dies to make a square tube without collapse and fit-contacting the mold during the whole pressing process (Fig. 1). Collapse of tube surface may be due to geometric effect, property of the material, and contact friction on symmetrical sections of the square tube. Since not much work had been carried out on squaring clad tubes, the main aim of this study was to establish incremental elastic-plastic finite-element analysis formulation of Coulomb's friction law and adopted $r_{\min}$ method of Yamada et al. (1968) to global stiffness matrix to solve the problems of contact friction, contact-separation of tube and die, limits of material element rotating increment allowance or strain increment allowance, and elastic-plastic transient situation in order to meet the demand of calculation for linear increment and acquire correct and complete boundary contact situation. Selectively reduced integration method (SRI) (Malkus et al., 1978) is also applied in this study. It has been proved to be effectively applied to incompressible materials as well as to deal with shell elements in finite-element analysis. Such method could be used in simulating the deformation history of squaring process of clad tubes, load distribution, and discussion on the influence of process parameters. As for the squaring defects of collapse (collapse ratio *C/t*, $C_m/t$, $\delta_1/t$, $\delta_2/t$, a measurement of the extent of collapse) and asymmetry (deviation ratio *C1/C2*), an

*Paper Received June, 2012. Revised September, 2012, Accepted October, 2012, Author for Correspondence: Tsung-Chia Chen.*

* *Professor, Department of Mechanical Engineering, National Chin-Yi University of Technology, Taichung, Taiwan 41170, ROC.*

** *Graduated Student, Department of Mechanical Engineering, National, Chin-Yi University of Technology, Taichung, Taiwan 41170, ROC.*

attempt is made to explore the effects of the process parameters, such as geometric ratio *R/t*, strain hardening exponent *n*, and friction coefficient $\mu$, on the formation. It is expected to make a complete square tube without squaring defects for a suitable set of process parameters. The above information is necessary for manufacturers and designers.

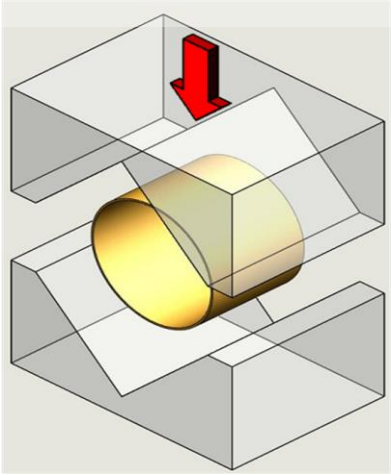

Fig. 1. Schematic diagram of the compression process of circle tube.

## BASIC THEORY

**Variational Principle**

The updated Lagrangian formulation (ULF) is based on the modified principle of virtual velocity (McMeeking et al., 1975):

$$\int_V \{(\sigma_{ij}^J - 2\sigma_{ik}D_{ik})\delta D_{ij} + \sigma_{jk}L_{ik}\delta L_{ij}\}dV = \int_{S_t} \dot{f}_i \delta v_i dS, \quad (1)$$

The derivation of this equation considers the fact that, for sheet metal forming, $\det(\partial x/\partial x_0) \cong 1$. Constitutive equations can be defined as a small strain, linear elasticity and the large deformation, rate-independent, work-hardening plasticity (Cao et al., 1989):

$$\sigma_{ij}^J = C_{ijkl}^{ep} D_{kl} = C_{ijkl}^{ep} L_{kl}, \quad (2)$$

where $C_{ijkl}^{ep}$ is the symmetric tangent constitutive matrix.

Substituting Eq. (2) into Eq. (1) yields the final form of the principle of virtual velocity:

$$\int_V \bar{C}_{ijkl} L_{kl} \delta L_{ij} dV = \int_{S_t} \dot{f}_i \delta v_i dS, \quad (3)$$

where, $\bar{C}_{ijkl} = C_{ijkl}^{ep} + \Omega_{ijkl}$;

$$\Omega_{ijkl} = \frac{1}{2}\left(\sigma_{jl}\delta_{ik} - \sigma_{ik}\delta_{jl} - \sigma_{il}\delta_{jk} - \sigma_{jk}\delta_{il}\right).$$

**Stiffness Equation**

Standard finite element discretization, and the introduction of an elemental shape function enable Eq. (3) to be replaced by a system of algebraic equations,

$$K\Delta u = \Delta F + \Delta C, \quad (4)$$

Where $K$ is the elastic-plastic stiffness matrix and $\Delta u$ represents the nodal displacement increment.

**Selective Reduced Integration Formulation**

The volume of a plastic medium is incompressible. Therefore, implementing the full integration technique for finite elements leads to over-strong constraint on thin plates. This phenomenon is caused by setting to zero the shear strains $\gamma_{xz}$ and $\gamma_{yz}$ during deformation (Hinton et al., 1984). The selective reduced integration (SRI) procedure has been proven to treat effectively such problems as those involving volumetrically stiff contribution (Hughes, 1987). The generalized formulation of SRI due to Hughes (1980) was used to develop the finite-element program in this study, which uses a four-node shell element.

**Weighting Factor $r_{min}$ for the Increment of Each Loading Step**

During each increment, the material is referred to its configuration at the beginning of the increment (updated Lagrangian scheme). The contact and separation conditions of nodes and the state of elements must remain invariable during the increment. In order to satisfy this requirement and to assure the accuracy of this explicit integration scheme (static explicit formulation), the weighting factor $r_{\min}$ proposed by Yamada et al. (1968) is used to treat the elastic-plastic and contact-separation problems to choose the size of the increment to keep linear relation. The size of each loading step is determined by the smallest value of the following five *r*-values, $r_{\min} = \text{MIN}(r_1, r_2, r_3, r_4, r_5)$:

$r_1$: To ascertain the equivalent stress of elastic element just reaches the current yield surface

$r_2$: To limit the largest equivalent strain increment to linear relation

$r_3$: To limit the rotation increment to linear relation

$r_4$: For making a free node just contact with the tools

$r_5$: For making a contact node just depart from the tool surface

The above is proved valid in the first order theory. More detailed information of weighting factor $r_{\min}$ can be found in (Leu, 1996).

**Unloading Process**

In order to know the final shape or the springback behavior, the unloading process is executed by assuming that all elements are reset to be

elastic. The force of the contact node is reversed to become the prescribed force boundary condition. All tools are removed for the elastic unloading procedure.

## NUMERICAL ANALYSIS

This work used a four-node rectangular shell element to derive a stiffness matrix. But in simulating squaring circular tube pressing process, the finite element meshes of the tools were triangular elements. The established tools and blank which employed CAD software were meshed and transferred into a data file. The elastic-plastic large deformation 3-D finite element method was used to perform numerical analysis. The simulated punch load-punch stroke and the results of the analysis were output to the CAD software to establish the figure.

Published material data of tubes (Leu, 2005), including the relations of equivalent stress and equivalent plastic strain for simulation, are shown in Table 1, in which one is a near ideal plastic material as a hard copper without hardening effect, and another is a low strength but work hardening material as a soft copper. Because of the symmetry of tubes, only a quarter portions of tools and the tube were modeled. The analyzed model of the squaring circular tube is shown in Fig. 2 in which (a) shows the profile of the punch head, the initial shape for simulation, (b) shows various boundary conditions of the deformed tube at a certain stage of squaring process, and (c) displays the deformation of the section in the central tube. The boundaries were altered as the loading proceeded; and, various friction coefficient $\mu$ were assumed in the calculation.

Table 1. Material properties of tubes for simulation.

| Material | Heat treatment | $n$ | $K$ / MPa | $\sigma_{0.2}$ / MPa |
|---|---|---|---|---|
| Hard copper | As received | 0.05 | 450 | 280 |
| Soft copper | 400℃ 1h | 0.46 | 610 | 50 |

$\bar{\sigma} = K\bar{\varepsilon}_p^n$, $E$ =135 MPa, $v$ =0.34, $\sigma_{0.2}$: yield stress by the offset method.

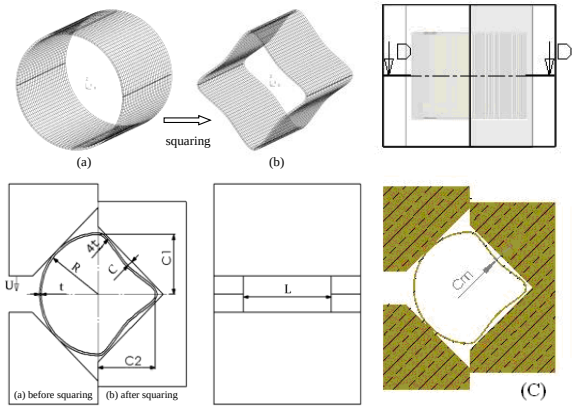


Fig. 2. Schematic representations of squaring tube showing (a) initial and (b) deformed conditions; (c) the deformation of the section in the central tube.

Fig. 3(a) presents rectangular elements when the tube was meshed. In simulating the squaring circular tube pressing process, appropriate boundary conditions must be imposed. Boundary conditions were set on the nodes such that the direction of rotation or displacement of nodes was constrained. In the simulation, the Y-axis's nodes of the tube on the XY-plane were constrained the displacement in the Z-direction and the rotation in the X-direction. Additionally, the Y-axis's nodes of the tube on the YZ-plane were constrained the displacement in the X-direction and the rotation in the Z-direction. Fig. 3(b) depicts the profile of the tube after the pressing process. $\delta_1$ stands for the collapse value on YZ-plane, and $\delta_2$ represents the collapse value on XY-plane. It aimed to discuss the effects of various parameters in the process, such as geometric ratio $R/t$, strain hardening exponent $n$, and friction coefficient $\mu$, on the occurrence of collapse (collapse ratio $C/t$, $C_m/t$, $\delta_1/t$, $\delta_2/t$, a measurement of the extent of collapse) and the extent of asymmetry (deviation ratio $C1/C2$) for the squaring circle tube process.

In the process of squaring circular tubes, the circular tube would contact with the punch head. Nodes contacting with or separated from tools need to be defined as contacting nodes and free nodes, respectively. Nodes not contacting with the tools are defined as free nodes and use the global coordinate (X, Y, Z); while the ones contacting with the tools are defined as contacting nodes and use local coordinate ($\xi$ ,$\eta$ ,$\zeta$ ), defined with right-hand law. Both Y and $\eta$ face inward. The contacting of each node would change with the deformation of the circular tube. In this case, the contacting nodes need to be examined the normal component of node force being less or equal to zero, when calculating the next displacement increment. When it is less or equal to zero, the boundaries of the node need to be changed to the boundaries of free nodes in the next displacement increment interval. The original free nodes then will need to be examined the geometric place being contacted with tools. If there is contact, the boundaries of the node are changed to the boundaries of contacting nodes in the next displacement increment interval. The above calculation is managed with extended $r_{\min}$ law.

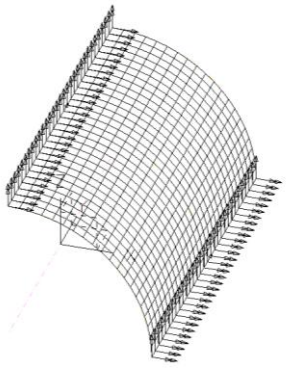

(a)

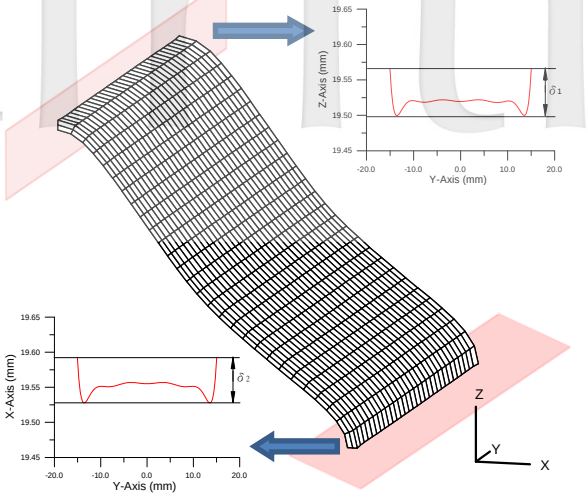


(b)

Fig. 3. (a) The mesh of tubes in squaring circular tube pressing simulation. (b) The profile of tube after squaring circular tube pressing process.

Both contact surfaces of circular tubes and tools are generated from intermittently alternation between sliding and sticking, which would occasionally result in computational difficulty. It is therefore important to deal with friction. Oden & Pries (1983) and Saran & Wagoner (1991) proposed revised Coulomb's friction law in which they presumed the friction containing sliding and sticking. This friction law is considered being able to effectively solve the computational difficulty caused by discontinuous change of the contact surface.

## RESULTS AND DISCUSSIONS

In the present work, the first part is to clarify the characteristics of squaring circular tube based on the analyzed model, such as the loading capacity, the processes of squaring deformation, the occurrence of collapse, and the extent of asymmetry. The second part is to explore the effect of the configuration of the clad tube on these squaring characteristics or defects, such as collapse and asymmetry.

### The Characteristics of Squaring Circular Tube

When proceeding compression in the squaring process and the contact points of load application moving out around the tube, it would have the effect of shortening the arm that has produced high moments; therefore the punch load can be further increased. In the meantime, the geometric constraints as a small edge radius produce in vertical and horizontal directions of diameter of tube, which will increase its degree with compression. If the material strain hardens in the plastic range, this effect will further increase the load carrying capacity under severe compression. Generally, the tube may be flattened in the contact zone of V-shape punch without separation; then a square tube would be successfully shaped. But in some processing conditions, separation would be occurred between punch and tube, and then a collapse would be occurred if the separation increases. The load capacity would turn to decrease with stroke. On the other hand, when the operation of squaring process proceeding in the vertical direction, an asymmetric section of square tube may be formed by severing contact friction as the induced friction force would push the material moving to the ends of diameter in the horizontal direction. In this case, *C2* must be larger than *C1*.

In order to verify the performance of the FE code, a published experimental data of squaring lateral compression of a copper tube carried out by Huang (2008) is predicted and shown in Fig. 4. The predicted punch load shows good agreement with that of the experiment, thereby demonstrating the reliability of the finite element model. Fig. 4 also displays that, when the tube is soft copper, the punch load is lower than it of hard copper in the beginning of formation; however, in the end of formation, the load for formation would rapidly increase after the soft copper generating reinforcing effect due to the load.

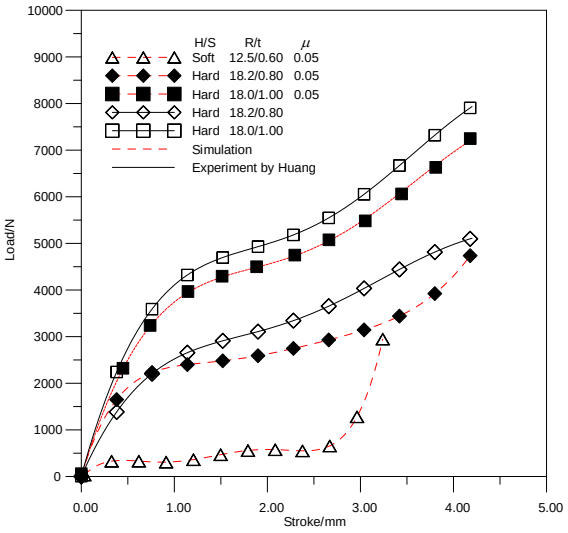


Fig. 4. Relations of punch load and punch stroke both experiment and prediction. ($L$ = 30.0mm)

Based on the present FE code, the squaring process for two kinds of tubes, hard and soft copper, were simulated to show the collapse, as shown in Fig. 5. The determination of final punch stroke for all simulations was based on the condition that the deformed edge of square tube was assumed to remain quarter circle. During the squaring compression process, the final punch stroke could be determined when the outer radius of edge was equal to four times tube-thickness ($4t$) in order to let the deformation state of squaring approach but to avoid the critical condition of pure bending in the present simulation.

In the figure, the deformed shapes of compressed tubes of hard and soft copper in the range of punch stroke (U) from 0.0mm to 3.24mm are shown to observe the formation of collapse for different heat treatment of material, annealing or not (soften or harden). From Fig. 5(a) & (b), the deformation of the tube end section could be observed. When the stroke reached 2.90mm, both soft and hard copper would present collapse, where separation occurred from the outset between the tube and the punch in the center of contact zone and increased its degree in the compression process. Observing the matter of stroke U = 2.90mm, it was clear that the geometry constraints were formed in the vertical and horizontal edges like a pure bending beam with two fix-like ends. Accordingly, all materials would move inwards around the tube and the extent of collapse would obviously increase in the compression process. It may show that the mechanism of collapse can be successfully traced in the simulation. Fig. 5(a) & (b) can be observed, after the springback, the tube end of hard copper tube over the tube end of soft copper tube with a larger collapse. In this case, soft copper tube was more appropriate to be made square tube. From above, collapse can be used to measure the formation of square tube. Fig. 5(c) depicts the contact of the punch and the circular tube in the process of squaring circular tube. It clearly presents the deformation of the circular tube till it is in the status of unload. As a result, the contact, the separation, and the friction in the compression process could be accurately calculated with $r_{min}$ law.

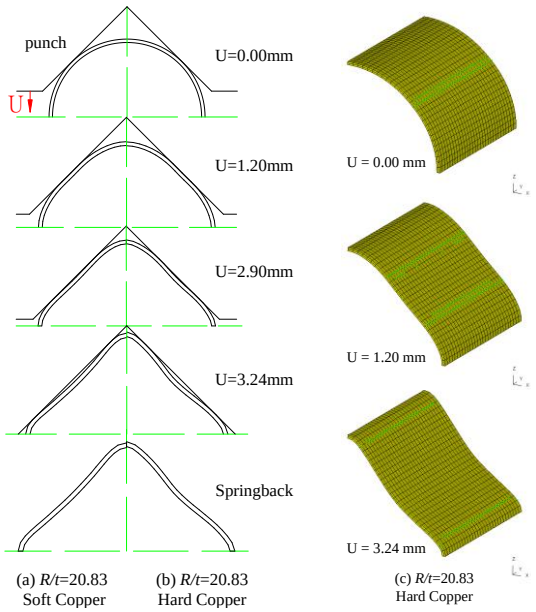


Fig. 5. Deformed geometries of squaring processes under the conditions of $R/t$ = 12.5/0.6, $L$ = 30.0mm and $\mu$ = 0.05, (a) the tube end section of soft copper, (b) the tube end section of hard copper, (c) depicts the contact of the punch and the circular tube in the process of squaring circular tube.

For the problem of collapse phenomenon as mentioned above shown in Fig. 5, a ratio $C/t$ called "the collapse ratio of the tube end section", in which $C$ represents the maximum distance of separation between punch and tube as shown in Fig. 2 and $t$ is the tube thickness, is defined to provide a measure of the formation of collapse as it can be used to represent the degree of collapse of squaring tube. $C_m/t$, on the other hand, stands for the "collapse ratio of the tube central section". Moreover, $\delta_1$ and $\delta_2$ in Fig. 3 represent the axial collapse on Y-Z plane and X-Y plane, respectively. $\delta_1/t$ and $\delta_2/t$ therefore are called the "axial collapse ratio". A larger $C/t$ indicates a larger extent of collapse. As the squaring compression proceeds, the deformation of edges in vertical and horizontal directions would produce different extents of deformation for the marked effects of contact friction and geometric constrain which would induce the asymmetric section of squared tube shown in Fig. 2(b). The extent of asymmetry would obviously increase with punch stroke in early stage as the material would move inwards (down) in vertical direction and outwards (right) in horizontal direction resulting from the tangential force induced by contact friction. Subsequently, the material in vertical edge would turn to move outwards (upper) for the geometric constrain in the horizontal edge increasing in the squaring compression process. Then the extent of asymmetry would turn to be reduced. Up to the final stage, the geometric constrains of both edges would grow enough to protect the material moving outwards, and then all materials would turn to move inwards resulting in the collapse. For the asymmetry of square tubes, a ratio $C1/C2$ called "deviation ratio" is defined to provide a measure of the asymmetry extent of the compressed tube.

For the squaring defects of asymmetry and collapse being affected by various process parameters, the simulations for exploring the effect of geometric ratio $R/t$ on the occurrence of collapse were carried out as shown in Fig. 6, and on the extent of asymmetry as shown in Fig. 7. These simulations were based on the case of hard copper tube shown in Table 1. Fig. 6 shows the effect of geometric ratio on the collapse ratio $C/t$. In Fig. 6, the $C/t$ slightly increases with $R/t$ ranging from 5.0 to 15.0 for various $n$ and $\mu$ and then strictly increases with $R/t$ when it is larger than 15.0. Nevertheless, with larger $\mu$, when $R/t$ reaches 25.0, $C/t$ is the maximum, and $C/t$ would then rapidly reduce with the increase of $R/t$. The turning point of $C/t$ is called "collapse critical point". From the figure, it is noted that a square tube without collapse could be successfully shaped in the case of small $R/t$. In Fig. 7, it shows that the greater extent of asymmetry would be produced in the case of large $\mu$ and small $n$ when $R/t$ equals 5.0. In the range of $R/t$ from 5.0 to 25.0, it is clear that the extent of asymmetry would increase (as decrease in the

figure) its degree as $\mu$ increases. In the same range of $R/t$, the extent of asymmetry would increase its degree as $n$ decreases in the cases of large $\mu$. When the $R/t$ larger than 25.0, all cases appear little effect on the asymmetry which all concentrate on the allowable error of five percentages as the upper region of dashed line shown in the figure.

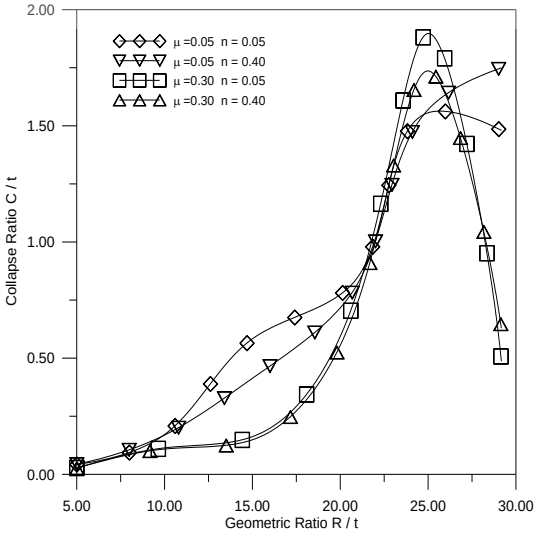


Fig. 6. The effect of geometric ratio $R/t$ on the collapse ratio $C/t$. ($L$ = 30.0mm)

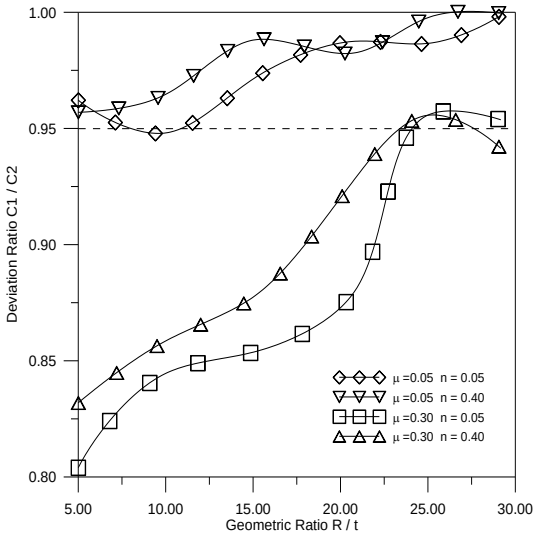


Fig. 7. The effect of geometric ratio $R/t$ on the deviation ratio $C1/C2$. ($L$ = 30.0mm)

**The Effects of the Configuration of Clad Tubes on the Squaring Characteristics**

According to the relation between geometry and collapse in previous section, when $R/t$ is small, either friction coefficient $\mu$ or strain hardening exponent $n$ would hardly affect collapse. When geometric ratio = 25, larger collapse is likely to occur. In this case, aiming at the geometric model with serious collapse ($R/t$ = 25), this section proposes to analyze six materials of soft and hard copper collocating with four clad tubes and fully soft and hard copper tubes for the optimal parameters. Configurations of clad tubes for simulations are shown in Table 2; Fig. 8 shows the distribution of clad tube. In order to successfully simulate the squaring compression process of clad tubes, a special feature on the simulation of the adhesive-bonded two-layer clad tubes subject to square tube is presented here to explore the effect of the configuration of the clad tube on the collapse and asymmetry behavior. The existence of complete adhesion with no peeling and no sliding at the interface between two layers of the clad tube is assumed in the calculation (Leu, 1999).

Table 2. Configurations of a copper clad tube for simulation.

| Type | $t_1$(C-H) | $t_2$(C-S) | $t_1$(C-S ) | $t_2$(C-H ) |
|---|---|---|---|---|
| C-H | 0.50 | 0.00 | | |
| C-HS1 | 0.25 | 0.25 | | |
| C-HS2 | 0.20 | 0.30 | | |
| C-S | | | 0.00 | 0.50 |
| C-SH1 | | | 0.25 | 0.25 |
| C-SH2 | | | 0.20 | 0.30 |

$t_1$ : thickness of the inner component metal of the clad copper tube, unit: mm.
$t_2$ : thickness of the outer component metal of the clad copper tube, unit: mm.
Thickness of the clad tube $t = t_1+t_2 = 0.5$mm.
Length of the clad tube $L$=30.0mm; Inner radius of the clad tube $R_i$=12.5mm.
Strain hardening exponent: C-H, $n$ = 0.05; C-S, $n$ = 0.46.
$E$ = 135GPa, $\mu$ = 0.05, $\upsilon$ = 0.34.

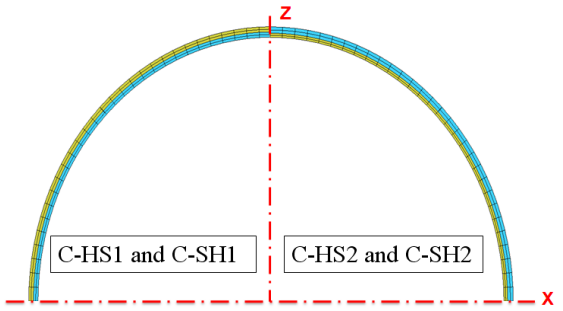


Fig. 8. Configurations of a copper clad tube for simulation.

Fig. 9 shows the relationship of punch load and punch stroke with different configurations of clad tube. The punch load generally increases with the amount of component metal C-H for its strength is larger than that of C-S. The punch loads of C-HS1 and C-SH1 (same configuration C-H/C-S=1) are almost consistent with each other, it is implied that the adhesion position (inner or outer) hardly affects the punch load. From the figure, when soft copper is the outer layer of the clad tubes (C-HS1 and C-HS2), the punch load would be higher than the outer layer being hard copper (C-SH1 and C-SH2). In general, the difference between the maximal punch load of clad tubes and fully soft copper is not significant.

Fig. 10 shows the distribution of stress in the squaring process of clad tubes. According to the figure, the maximal stress of the square tube would appear on the inner layer of the tube after springback and locate in the area with serious collapse. Fig. 10(c)

and 10(d) display the distribution of stress, from which the larger stress of clad tubes would concentrate on the inner hard copper, while the stress on the outer soft copper is smaller. According to the distribution of stress, the residual stress after the squaring process of clad tube has been remarkably improved. The maximal stress 390.59MPa appears on the configuration of C-H fully hard copper, while C-HS2 presents the minimal stress 362.23Mpa. C-HS2 is the analysis configuration of hard copper with 0.2mm inner thickness and soft copper with 0.3mm outer thickness. Overall speaking, the maximal stress would reduce with the decease of the inner thickness of hard copper. When the inner material is changed into soft copper, the above result would be obtained, Fig. 11. In this kind of configuration, the maximal residual stress would appear on C-SH2 configuration with 0.2mm-thick inner soft copper and 0.3mm-thick outer hard copper. From Fig. 10(c) and Fig. 11(c) (configuration C-H/C-S=1), the residual stress of the configuration with inner soft copper and outer hard copper (C-SH1) is less than the one with inner hard copper and outer soft copper (C-HS1). In both configurations, the maximal stress appears on hard copper as the forming force in harder material is higher than it in soft material.

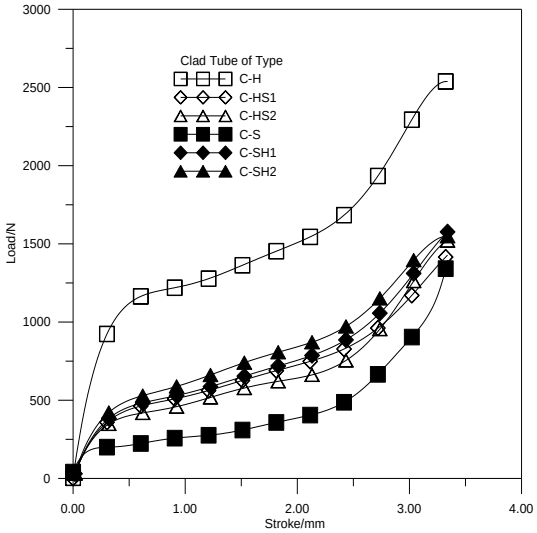


Fig. 9. Relations of punch load and punch stroke with different configurations of the clad tube. ($L$ = 30.0mm)

Fig. 12(a) shows the relationship between collapse ratio $C/t$ of the tube end section and configurations of the clad tube shown in Table 2. Fig. 12(b) shows the relationship between collapse ratio $C_m/t$ of the tube central section and configurations of the clad tube. From Fig.12, the least collapse in the beginning of formation appears on fully soft copper (C-S). However, the less collapse appears on the clad tubes in the final formation with punch stroke 3.34mm. After unload springback, the situation is the same that the collapse ratio before springback is larger than it after springback. From Fig. 12(a) and (b), the collapse ratio ($C/t$ and $C_m/t$) of the clad tube with outer soft copper is smaller than the one with outer hard copper. It is because the soft material is easier to stick on the tools surface so that the collapse would be improved. In general, the use of clad tubes in squaring process could effectively reduce collapse ratio ($C/t$ and $C_m/t$), particularly for outer soft copper.

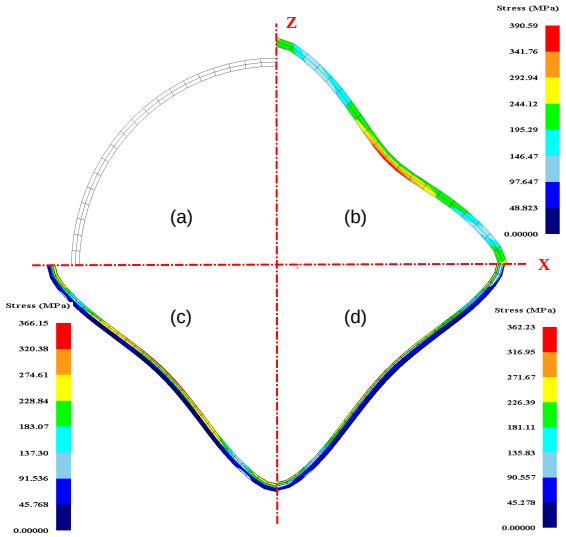


Fig. 10. The distribution of stress in the squaring process of clad tubes. (a) The initial shape of clad tube. (b) The stress distribution of C-H. (c) The stress distribution of C-HS1. (d) The stress distribution of C-HS2.

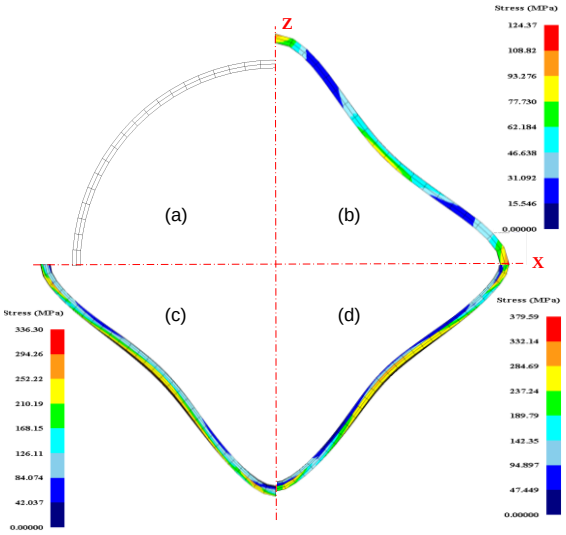


Fig. 11. The distribution of stress in the squaring process of clad tubes. (a) The initial shape of clad tube. (b) The stress distribution of C-S. (c) The stress distribution of C-SH1. (d) The stress distribution of C-SH2.

Fig. 13(a) shows the relationship between axial collapse ratio $\delta_1/t$ of the Y-Z plane and configurations of the clad tube shown in Table 2. Fig. 13(b) shows

the relationship between axial collapse ratio $\delta_2/t$ of the X-Y plane and configurations of the clad tube. From Fig. 13, $\delta_1/t$ and $\delta_2/t$ would increase with the increase of punch stroke till the final stage (3.34mm). Besides, the use of clad tube could effectively reduce axial collapse ratio. What is more, clad tube with outer soft copper, Fig. 13(a) & (b), would present less axial collapse ratio than the one with outer hard copper.

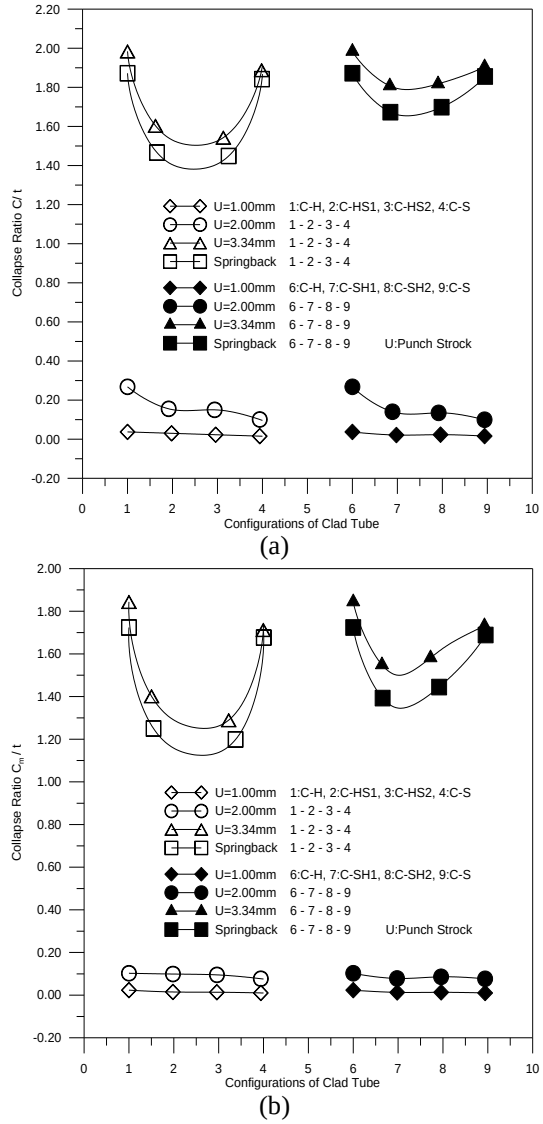


Fig. 12. (a) Relations of collapse ratio $C/t$ of the tube end section and configurations of the clad tube with different punch strokes. (b) Relations of collapse ratio $C_m/t$ of the tube central section and configurations of the clad tube with different punch strokes. ($L$ = 30.0mm).

Fig. 14 shows the relationship between deviation ratio *C1/C2* and configurations of the clad tube shown in Table 2. After unloading, when the thickness of soft copper in clad tube with various thicknesses increases, the extent of asymmetry would decrease. In this case, ones with higher soft copper are likely to form symmetric square tubes.

As in the above discussion, it must be recalled that these process parameters interact and cannot strictly be considered in isolation.

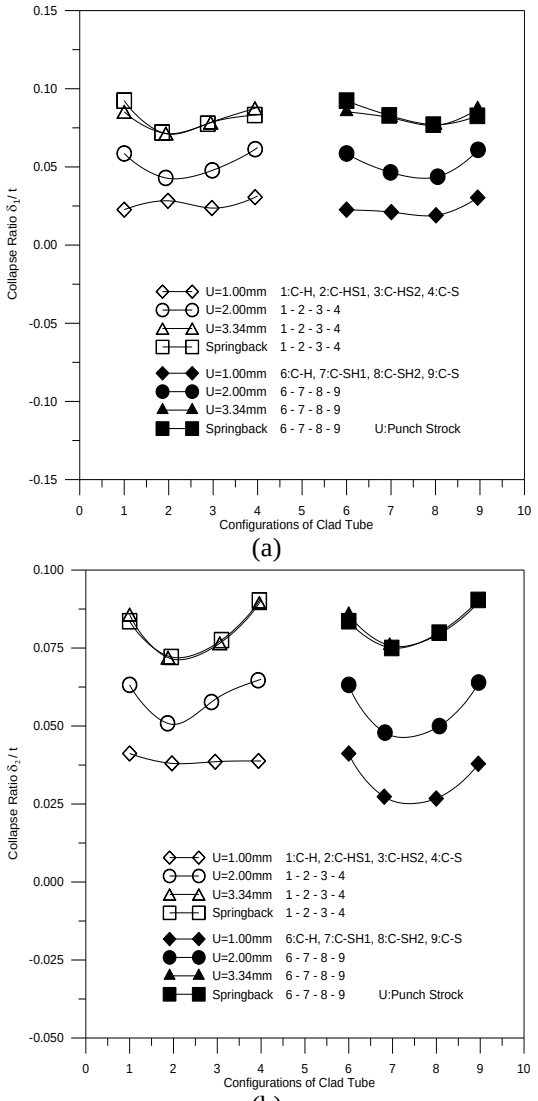


Fig. 13. (a) Relations of axial collapse ratio $\delta_1/t$ of the Y-Z plane and configurations of the clad tube with different punch strokes. (b) Relations of axial collapse ratio $\delta_2/t$ of the X-Y plane and configurations of the clad tube with different punch strokes. ($L$ = 30.0mm)

## CONCLUSIONS

A 3-D elastic-plastic finite-element model based on an updated Lagrangian formulation is developed to simulate punch load and deformed geometries in the squaring process of clad circular tube. Based on the $r_{\min}$ technique, formulation and algorithms are developed to treat the nonlinear problems of deformation dependence in an

incremental way, such as the geometric changes, the sliding-sticking friction, the inelastic constitutive behavior, and the contact-separation boundary problems.

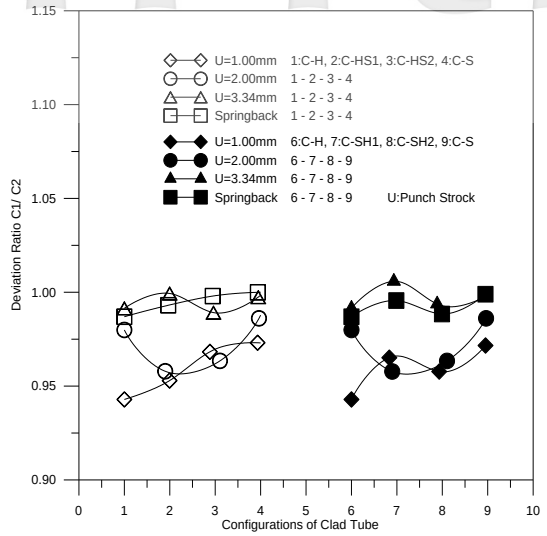


Fig. 14. Relations of deviation ratio *C1/C2* and configurations of the clad tube with different punch strokes. ($L$ = 30.0mm)

The calculated punch load of compression agrees with published experimental results. It demonstrates the applicability and reliability of the present FE model. The characteristics of squaring process, such as collapse and asymmetry, are simulated and reported in a theoretical manner. A special feature of the present work is to investigate the effects of various process parameters on the occurrence of collapse and the extent of asymmetry in the squaring process of clad circular tubes. The conclusions are summarized as follows.

1. With finite element analysis, the deformation in the squaring process of circular tubes can be accurately analyzed, meaning that the entire deforming process could be successfully drawn out.
2. Geometric ratio presents the largest effect on collapse ratio that the larger the geometric ratio, the larger the collapse ratio. Nevertheless, when geometric ratio exceeds 25, the collapse ratio would rapidly decline that the square tube without deformation would be more easily produced. When $R/t$ is less than 25, friction coefficient $\mu$ and strain hardening exponent $n$ do not show much effect on collapse ratio.
3. The symmetric square tube could be successfully made in the large geometric ratio $R/t$ and small friction coefficient $\mu$ under the allowable error of five percent in view of engineering. The strain hardening exponent $n$ obviously affects the extent of asymmetry in the squaring process only under the case of small geometric ratio $R/t$ and large friction coefficient $\mu$.
4. Clad tubes with soft and hard copper could effectively improve the collapse ratio in $R/t$ = 25 and reduce punch load. With the six configurations, the collapse ratio of C-HS (inner hard copper, and outer soft copper) is the least; and this kind of square tubes would present better symmetry.

The discussion outlined above may help understand the characteristics of squaring process for shaping a square tube without collapse or asymmetry.

## ACKNOWLEDGMENT

This paper was supported by the National Science Council, Taiwan, Republic of China, through Grant NSC 98-2221-E-167-001. We are grateful to the National Center for High-performance Computing for computer time and facilities.

## REFERENCES

Cao, H.L., and Teodosiu, C., "Finite element calculation of springback effects and residual stress after 2D deep drawing," *Conference proceedings: Computational Plasticity - fundamentals and applications*, Barcelona, Spain (1989).

DeRuntz, J.A., and Hodge, P.G., Crushing of a tube between rigid plates," *Transactions of ASME, Journal of Applied Mechanics*, Vol.30, pp.391-395 (1963).

Gotoh, M., and Shibada, Y., "Elasto-plastic finite element analysis for one and two dimensions of lateral compression of tube," *Spring Proceeding Plastic Working*, Cho-Fu, Tokyo (1989).

Hinton, E., and Owen, D.R., "*Finite Element Software for Plates and Shell*," Swansea, UK: Pineridge (1984).

Huang, Y.M., "Elasto-plastic finite element analysis of squaring circular tube," *Transactions of Nonferrous Metal Society of China*, Vol.18, pp.665-673 (2008).

Huang, Y.M., "Finite element analysis of tube inward curling process by conical dies," *Journal of Materials Processing Technology*, Vol.170, pp.616-623 (2005).

Hughes, T.J.R., "Generalization of selective integration procedures to anisotropic and nonlinear media," *International Journal for Numerical Methods in Engineering*, Vol.15, No.9, pp.1413-1418 (1980).

Hughes, T.J.R., "*The Finite Element Method*," Englewood Cliffs, NJ: Prentice-Hall (1987).

Johnson, W., Reid, S.R., and Reddy, T.Y., "The compression of crossed layers of thin tubes," *International Journal of Mechanical Sciences*, Vol.19, pp.423-437 (1977).

Leu, D.K., "Finite element simulation of the squaring circular tube," *International Journal of Advanced Manufacturing Technology*, Vol.25,

pp.691-699 (2005).
Leu, D.K., "Finite-element simulation of hole-flanging process of circular sheets of anisotropic materials," *International Journal of Mechanical Sciences*, Vol.38, No.8-9, pp.917-933 (1996).
Leu, D.K., "Finite-element simulation of the lateral compression of aluminium tube between rigid plates," *International Journal of Mechanical Sciences*, Vol.41, pp. 621-638 (1999).
Leu, D.K., "The curling characteristics of static inside-out inversion of metal tubes," *International Journal of Machine Tools and Manufacture*, Vol.40, pp.65-80 (2000).
Leu, D.K., "The shaping of a circular tube into a symmetric square-tube by finite-element modeling," *Journal of Materials Processing Technology*, Vol.178, pp.287-296 (2006).
Lin, J.F., Li, F., Yuan, S.J., and Han, J.C., "Research on Hydroforming Tubular Parts with Dissymmetrical Structure," *Journal of the Chinese Society of Mechanical Engineers*, Vol.31, No.4, pp.335-339 (2010).
Malkus, D.S., and Hughes, T.J.R., "Mixed finite-element methods-reduced and selective integration techniques: a unification of concepts," *Computer Methods in Applied Mechanics and Engineering*, Vol.15, No.1, pp.63-81 (1978).
McMeeking, R.M., and Rice, J.R., "Finite-element formulations for problems of large elastic-plastic deformation," *International Journal of Solids and Structures*, Vol.11, pp.601-616 (1975).
Miscow, F.P.C., and Al-Qureshi, H.A., "Mechanics of static and dynamic inversion process," *International Journal of Mechanical Sciences*, Vol.39, No.2, pp.147-161 (1997).
Mutchler, L.D., "Energy absorption of aluminium tubing," *Transactions of ASME, Journal of Applied Mechanics*, Vol.27, pp.740-743 (1960).
Oden, J.T., and Pries, E.B., "Nonlocal and nonlinear friction laws and variational principles for contact problems in elasticity," *Transactions of ASME, Journal of Applied Mechanics*, Vol.50, No.1, pp.67-76 (1983).
Reid, S.R., and Reddy, T.Y., "Effect of strain hardening on the lateral compression of tubes between rigid plates," *International Journal of Solids and Structures*, Vol.14, pp.213-225 (1978).
Reid, S.R., Drew, S.L.K., and Carney, J.F., III, "Energy absorbing capacities of braced metal tubes," *International Journal of Mechanical Sciences*, Vol.25, No.9-10, pp.649-667 (1983).
Saran, M.J., and Wagoner, R.H., "Consistent implicit formulation for nonlinear finite element modeling with contact and friction. Part I. Theory," *Transactions of ASME, Journal of Applied Mechanics*, Vol.58, No.2, pp.499-506 (1991).
Watson, A.R., Reid, S.R., Johnson, W., and Thomas, S.G., "Large deformations of thin-walled circular tubes under transverse loading (II)," *International Journal of Mechanical Sciences*, Vol.18, pp.387-397 (1976).
Watson, A.R., Reid, S.R., Johnson, W., and Thomas, S.G., "Large deformations of thin-walled circular tubes under transverse loading (III)," *International Journal of Mechanical Sciences*, Vol.18, pp.501-509 (1976).
Yamada, Y., Yoshimura, N., and Sakurai, T., "Plastic stress-strain matrix and its application for the solution of elastic-plastic problems by the finite-element method," *International Journal of Mechanical Sciences*, Vol.10, pp.343-354 (1968).
Yu, H.P., and Li, C.F., "Finite element analysis of free expansion of aluminum alloy tube under magnetic pressure," *Transactions of Nonferrous Metals Society of China*, Vol.15, No.5, pp.1040-1044 (2005).
Zhang, Z.C., Manabe, K., Zhu, F.X., Mirzai, M.A., and Li, T.H., "Evaluation of Hydroformability of TRIP Steel Tube by Flaring Test," *Journal of the Chinese Society of Mechanical Engineers*, Vol.31, No.5, pp.375-382 (2010).

# V 型模具側向壓縮複合管之有限元素分析

陳聰嘉　葉峻銘
國立勤益科技大學 機械工程系

## 摘 要

複合管的側向壓縮製程是屬於塑性大變形，本文運用 updated Lagrangian formulation (ULF)觀念，結合滑動-黏滯摩擦方法，建立增量型彈塑性有限元素分析程式，驗證複合管的側向壓縮製程，並於設計階段，預測複合管側向壓縮後的挫屈及不對稱。製程參數(幾何比 *R/t*，摩擦係數 $\mu$ 和應變硬化指數 *n*)對圓管側向壓縮製程之影響，經模擬分析發現幾何比對圓管側向壓縮製程影響最明顯，當 *R/t*=25 時，挫屈最容易發生。本文針對幾何比 *R/t*=25 的圓管，提出六種軟硬材料搭配而成之複合圓，進行模擬分析，發現複合管可有效改善圓管側向壓縮後的挫屈及不對稱。由此可證明本計算法，能夠有效地模擬圓管側向壓縮製程。